Chinese Chemical Letters 33 (2022) 3217–3220

Contents lists available at ScienceDirect

Chinese Chemical Letters

journal homepage: www.elsevier.com/locate/cclet

Ultrathin FeS nanosheets with high chemodynamic activity for sensitive colorimetric detection of H_2O_2 and glutathione

Yefan Duan[a,1], Qi Li[a,1], Panpan He[a,1], Yan Li[a], Jingrun Song[a], Jing Wang[a], Junjie Liu[a], Jiang Zhou[b,*], Fei Chen[c], Zhusheng Huang[a], Jianfei Sun[d], Ying Zhang[a,*], Zhimin Luo[a,*]

[a] State Key Laboratory for Organic Electronics and Information Displays & Jiangsu Key Laboratory for Biosensors, Institute of Advanced Materials (IAM), Jiangsu National Synergetic Innovation Center for Advanced Materials (SICAM), College of Electronic and Optical Engineering & College of Microelectronics, Nanjing University of Posts and Telecommunications, Nanjing 210023, China
[b] Ningbo Medical Center Li Huili Hospital, Ningbo 315040, China
[c] Laboratory of Polymer Materials and Engineering, NingboTech University, Zhejiang University, Ningbo 315100, China
[d] State Key Laboratory of Bioelectronics, Jiangsu Laboratory for Biomaterials and Devices, Department of Biological Science and Medical Engineering, Southeast University, Nanjing 210009, China

ARTICLE INFO

Article history:
Received 1 September 2021
Revised 10 October 2021
Accepted 15 October 2021
Available online 21 October 2021

Keywords:
FeS nanosheets
Chemodynamic activity
Colorimetric biosensors
Hydrogen peroxide
Glutathione

ABSTRACT

Iron chalcogenides have attracted great interest as potential substitutes of nature enzymes in the colorimetric biological sensing due to their unique chemodynamic characteristics. Herein, we report the preparation of ultrathin FeS nanosheets (NSs) by a simple one-pot hydrothermal method and the prepared FeS NSs exhibit strong Fenton-reaction activity to catalyze hydrogen peroxide (H_2O_2) for generation of hydroxyl radical (•OH). Based on the chromogenic reaction of resultant •OH with 3,3′,5,5′-tetramethylbenzidine (TMB), we develop colorimetric biosensors for highly sensitive detection of H_2O_2 and glutathione (GSH). The fabricated biosensors show wide linear ranges for the detection of H_2O_2 (5–150 μmol/L) and GSH (5–50 μmol/L). Their detection limits for H_2O_2 and GSH reach as low as 0.19 μmol/L and 0.14 μmol/L, respectively. The experimental results of sensing intracellular H_2O_2 and GSH demonstrate that this colorimetric method can realize the accurate detection of H_2O_2 and GSH in normal cells (L02 and 3T3) and cancer cells (MCF-7 and HeLa). Our results have demonstrated that the synthesized FeS NSs is a promising material to construct colorimetric biosensors for the sensitive detection of H_2O_2 and GSH, holding great promising for medical diagnosis in cancer therapy.

Hydrogen peroxide (H_2O_2) is an important molecule in the living process, which is related to many diseases such as inflammatory, diabetes, cardiovascular diseases and cancers [1–3]. Glutathione (GSH), a kind of endogenous antioxidant in human intracellular and extracellular fluids, can eliminate free radicals from body and is associated with a variety of clinical diseases [4–6]. H_2O_2 and GSH are generally used as key biomarkers and prognostic indicators in the biomedical diagnosis. Currently, many analytical methods have been developed to determine H_2O_2 and GSH [1,4–6]. Colorimetric method attracts great attention due to its characteristics of simplicity, rapidity, cost-effectiveness, visualizability and strong universality [7–9]. However, most of colorimetric determination kits for the detection of H_2O_2 and GSH are composed of horseradish peroxidase and glutathione reductase, which have the shortcomings of time-consuming synthesis, easy denaturation and high cost [1,10]. Exploration of substitutes with high catalytic or Fenton-reaction activity like horseradish peroxidase and glutathione reductase is necessary for widening applications of colorimetric method to detect H_2O_2 and GSH.

Two-dimensional (2D) nanomaterials have attracted considerable attention in biological applications in the last decade [11–15]. 2D transition metal chalcogenides, *e.g.*, Co_9S_8 [16], $MoSe_2$ [17], MoS_2 [18], WS_2 [19] and VS_2 [20], have been found to possess the intrinsic peroxidase-like catalytic activity, which can serve as enzyme mimics for the colorimetric detection of H_2O_2 and GSH. Besides, iron-based chalcogenides have been also discovered to have Fenton-reaction characteristics [21,22]. They can react with H_2O_2 to produce hydroxyl radical (•OH), which oxidates 3,3′,5,5′-tetramethylbenzidine (TMB) into a blue compound. Fenton-reaction property of these iron-based chalcogenides makes them promising for colorimetric determination kits in the detec-

* Corresponding authors.
E-mail addresses: jiang_zhou1979@163.com (J. Zhou), yingzhang@njupt.edu.cn (Y. Zhang), iamzmluo@njupt.edu.cn (Z. Luo).
[1] These authors contributed equally to this work.

https://doi.org/10.1016/j.cclet.2021.10.041
1001-8417/

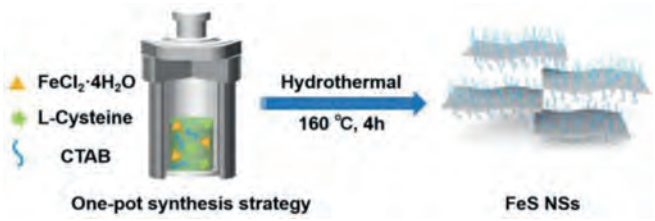

Scheme 1. One-pot hydrothermal synthesis of ultrathin FeS NSs.

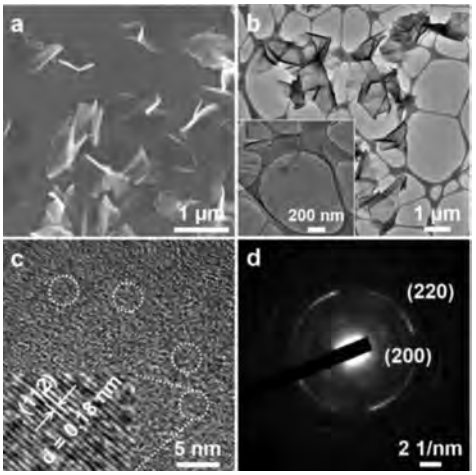

Fig. 1. (a) SEM and (b) TEM images of FeS NSs. Inset in (b): The partially enlarged TEM image of FeS NSs. (c) HRTEM image and (d) SAED pattern of FeS NSs.

tion of H_2O_2 and GSH. Although previous reports have demonstrated that iron-based chalcogenides can be used for colorimetric sensing of H_2O_2 and GSH [21], no one has reported the synthesis of 2D iron-based chalcogenides for colorimetric sensing of H_2O_2 and GSH.

In this work, ultrathin 2D FeS nanosheets (NSs) are prepared by a simple one-pot hydrothermal method by using hexadecyltrimethylammonium bromide (CTAB) as a surfactant. The Fenton-reaction characteristics of FeS NSs are investigated for further construction of colorimetric biosensors to detect H_2O_2 and GSH. The fabricated colorimetric biosensors based on FeS NSs can sensitively monitor H_2O_2 and GSH levels in the normal and cancer cells. This simple and cost-effective colorimetric FeS NS-based sensor holds great potential in the clinical diagnosis.

FeS NSs were synthesized by a simple one-pot hydrothermal method by using $FeCl_2{\cdot}4H_2O$ and L-cysteine as precursors and CTAB as a surfactant (Scheme 1). CTAB has been widely used as a surfactant for the synthesis of ultrathin 2D nanomaterials. The prepared product was characterized by TEM, HRTEM, SEM, AFM, XPS, XRD and Raman spectroscopy. It can be observed from the SEM (Fig. 1a) and TEM (Fig. 1b) images that the product has 2D morphology with an average lateral size of ~1 μm. AFM image (Fig. S1 in Supporting information) gives its thickness of less than 3 nm, indicating their ultrathin structure. HRTEM image in Fig. 1c displays the crystal fringe spacing of 0.18 nm corresponding to the (112) crystal plane of FeS [23]. The corresponding selected area electron diffraction (SAED) pattern (Fig. 1d) shows two diffraction rings corresponding to the (220) and (200) crystal planes of FeS [24].

XRD and Raman spectroscopy were used to study the structure of product. XRD pattern (Fig. 2a) exhibits typical diffraction peak of 17.5°, which is in accordance with the (001) crystal plane of tetragonal-phase FeS [25]. Raman peaks at 221 and 283 cm^{-1} (Fig. 2b) are attributed to the B_{1g} and A_{1g} modes of FeS, and Raman peak at 398 cm^{-1} (Fig. 2b) is attributed to the weak oxidation of FeS [26–28]. In order to further determine the chemical composition of product, XPS characterization was performed. Survey XPS spectrum of product (Fig. S2 in Supporting information) shows obvious binding energy peaks of Fe (~720.0 eV), O (~530.0 eV), N (~401.0 eV), C (~283.6 eV) and S (~162.0 eV) elements. Two primary binding energy peaks at 711.3 and 724.9 eV in the high-resolution Fe 2p XPS spectrum (Fig. 2c) are attributed to Fe $2p_{3/2}$ and Fe $2p_{1/2}$ of Fe^{2+} [29,30]. High-resolution S 2p XPS spectrum (Fig. 2d) shows the two binding energy peaks at 160.8 and 161.9 eV corresponding to S $2p_{3/2}$ and S $2p_{1/2}$ of S^{2-} [31]. All the above characterizations prove the successful preparation of FeS NSs.

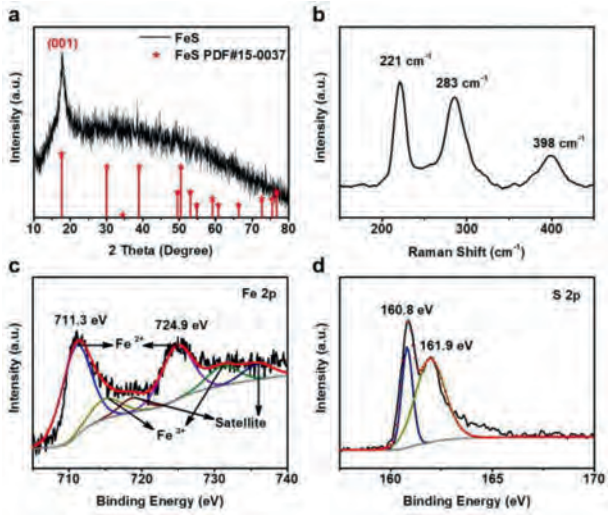

Fig. 2. (a) XRD pattern and (b) Raman spectrum of FeS NSs. High-resolution (c) Fe 2p and (d) S 2p XPS spectra of FeS NSs.

Chemodynamic characteristics of FeS NSs was explored by their Fenton reaction with H_2O_2 to produce $^{\bullet}OH$, which can oxidate TMB to form blue oxidized TMB (oxTMB) (Fig. S3a in Supporting information). When FeS NSs were added into the mixture of TMB and H_2O_2, the color of mixed solution will turn blue and a characteristic absorption peak at 652 nm can be observed (Fig. S3b in Supporting information). As a control, there is no change of color and absorbance for the solution containing only TMB or H_2O_2 (Fig. S3b). If GSH is added into the reaction system containing FeS NSs, TMB and H_2O_2, the color of blue oxTMB fades into colorlessness and its absorbance at 652 nm sharply decreases (Fig. S3b). These results indicate that FeS NSs have evident Fenton-reaction activity and are promising to provide a feasibility to construct colorimetric biosensors for sensitive detection of H_2O_2 and GSH.

Several influence factors such as the concentration of FeS NSs, pH value, reaction temperature and time were investigated in order to optimize the conditions of Fenton reaction. As shown in Fig. S4a (Supporting information), the color of the mixed solution containing FeS NSs, TMB and H_2O_2 gradually deepens and the absorbance at 652 nm increases with the increasing concentration of FeS NSs, which means that the Fenton reaction of FeS NSs is concentration-dependent. 0.4 μg/mL of FeS NSs is chosen as the most suitable concentration applied in the following experiments. The influence of pH value on the chromogenic reaction was studied. Different HAC–NaAC buffer solutions (pH = 2.0, 3.0, 4.0, 5.0, 6.0 and 7.0) were taken as the reaction system, respectively. As shown in Fig. S4b (Supporting information), the absorbance at 652 nm of reaction system reaches the highest value at pH 4.0. It can be explained that H_2O_2 prefers to decompose into H_2O and O_2 rather than $^{\bullet}OH$ at the higher pH value (pH > 5.0) and the gen-

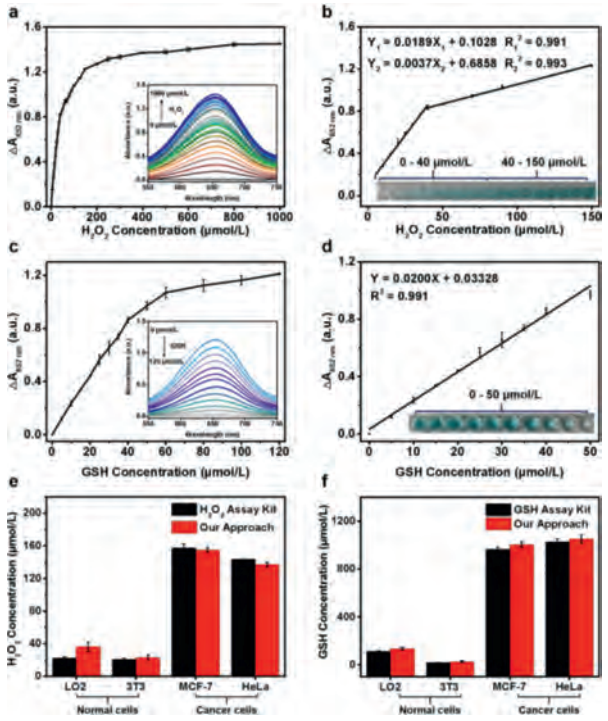

Fig. 3. (a) The absorbance enhancement ($\triangle A_{652\ nm} = A - A_0$) of FeS NSs (0.4 μg/mL) and TMB (0.2 mmol/L) with different concentrations of H_2O_2 at pH 4.0. Inset: the UV–vis-NIR absorption curves with increasing concentrations of H_2O_2. A and A_0 are the absorbance of FeS NSs and TMB with and without H_2O_2, respectively. (b) The linear calibration plots for sensing H_2O_2. Inset: photographs of corresponding samples. (c) The absorbance enhancement ($\triangle A'_{652\ nm} = A'_0 - A'$) of FeS NSs (0.4 μg/mL) with TMB (0.2 mmol/L) and H_2O_2 (0.1 mmol/L) in the presence of different concentrations of GSH at pH 4.0. Inset: the UV–vis-NIR absorption curves with increasing concentrations of GSH. A'_0 and A' are the absorbance of reaction system without and with GSH, respectively. (d) The linear calibration plots for sensing GSH. Inset: photographs of corresponding samples. (e) H_2O_2 and (f) GSH levels of normal cell (L02 and 3T3) and cancer cells (MCF-7 and HeLa) evaluated by the commercial H_2O_2 assay kit and FeS NSs.

erated O_2 can restrain the oxidation of TMB [32,33]. The influence of different temperatures (25, 30, 35, 40, 45, 50 and 60 °C) on the Fenton-reaction was explored. As shown in Fig. S4c (Supporting information), the absorbance at 652 nm of reaction system gradually increases with rising temperature from 25 °C to 45 °C. When the reaction temperature is up to 45 °C, the absorbance at 652 nm of reaction system reaches the highest value, indicating that the optimal temperature of Fenton reaction for FeS NSs is about 45 °C. Different incubation time was further performed to investigate its effect on the Fenton reaction. As shown in Fig. S4d (Supporting information), it can be seen that the optimal incubation time for Fenton reaction is 50 min. Based on thorough investigation of the Fenton-reaction conditions, the maximum Fenton-reaction activity of FeS NSs (0.4 μg/mL) is observed at pH 4.0 after incubation at 45 °C for 50 min.

A colorimetric method based on FeS NSs is used to detect H_2O_2 and GSH under the optimized conditions. As shown in Fig. 3a, the absorbance of reaction system at 652 nm increases with the concentration of H_2O_2 less than 150 μmol/L. An evident change of the absorbance of reaction system at 652 nm can be monitored even though the amount of H_2O_2 is trace (inset in Fig. 3b). The absorbance of reaction system at 652 nm presents good linear relationships with the concentration of H_2O_2 within a range from 5 μmol/L to 150 μmol/L (Fig. 3b). The first linear relationship is fitted at 5–40 μmol/L ($Y_1 = 0.0189\ X_1 + 0.1028$, $R_1^2 = 0.991$) and the second linear relationship is fitted at 40–150 μmol/L ($Y_2 = 0.0037\ X_2 + 0.6858$, $R_2^2 = 0.993$). LOD of colorimetric method based on FeS NSs is evaluated to be 0.19 μmol/L. Compared to the previously reported colorimetric methods based on other nanomaterials (Table S1 in Supporting information) [21,34–38], our constructed FeS NSs-based colorimetric method exhibits more advantages including wider linear range (5–150 μmol/L) and lower detection limit (0.19 μmol/L).

GSH is the most abundant tripeptide in cells. Abnormal concentration of GSH can lead to cancer, cardiovascular disease, Alzheime and other serious diseases [39,40]. Therefore, it is of great significance to develop a simple and effective biosensor to detect GSH. To evaluate the assay sensitivity of colorimetric method based on FeS NSs, different concentrations of GSH (0–120 μmol/L) were added into the mixed solution containing FeS NSs, TMB and H_2O_2, and then incubated for 50 min at 45 °C to measure the absorbance of reaction system at 652 nm. The reductive GSH can reduce oxTMB to colorless TMB and this process is accompanied by decreasing the absorbance of oxTMB at 652 nm. It is worth noting that the addition of trace amount of GSH can cause a significant decrease of the absorbance of oxTMB. The decrease of its absorbance ($\triangle A'_{652\ nm}$) has a good linear relationship with the GSH concentration range from 5 μmol/L to 50 μmol/L ($Y_3 = 0.0200\ X_3 + 0.03328$, $R_3^2 = 0.991$) (Figs. 3c and d), and LOD is calculated to be 0.14 μmol/L. This analytical performance is superior to that of reported sensing platform based on Fe_3O_4 nanoparticles [41], Co_3O_4 nanocrystals [42], Au nanoparticles [43], Au nanoclusters [44], carbon nanodots [45] or FeS_2 nanoparticles (Table S2 in Supporting information) [21]. The gradual fading of blue color of oxTMB with the addition of GSH is visible to naked eyes (inset in Fig. 3d), indicating that FeS NSs can be applied in a simple colorimetric method of visually observed assay for the detection of GSH.

Normal and cancer cells are different in the microenvironment [46–48]. The concentration of H_2O_2 in cancer cells is often at the micromole level [49–51], while the concentration range of GSH as the biomarker for cancer is generally from 1 mmol/L to 10 mmol/L [52,53]. It is of great significance to develop a simple method to detect H_2O_2 and GSH levels in cells. The good linear range and low LOD of our approach make it be able to satisfy the detection of H_2O_2 and GSH levels in normal cells and cancer cells. In order to quantitative analysis of intracellular H_2O_2 and GSH levels based on our method, four cells including two normal cells (L02 and 3T3) and two cancer cells (MCF-7 and HeLa) are chosen as models. As shown in Fig. 3e, the H_2O_2 levels in L02, 3T3, MCF-7 and HeLa cells are evaluated by our colorimetric method based on FeS NSs to be 36, 23, 156 and 138 μmol/L, respectively. Meanwhile, The GSH levels in L02, 3T3, MCF-7 and HeLa cells are measured by our colorimetric method to be 134, 25, 1009 and 1058 μmol/L, respectively (Fig. 3f). Our measured data show a high degree of agreement with those evaluated by commercial assay kits (Figs. 3e and f), suggesting the accuracy and reliability of colorimetric sensing method based on FeS NSs for the detection of intracellular H_2O_2 and GSH levels both in normal cells and cancer cells. Compared with sensing method by using commercial assay kits, colorimetric method based on FeS NSs is more cost-effective.

In summary, ultrathin FeS NSs have been synthesized by one-pot hydrothermal method, which possess excellent Fenton-reaction activity to decompose H_2O_2 into $^{\bullet}OH$. Based on the outstanding chemodynamic characteristics of FeS NSs, a new colorimetric sensor has been constructed for rapidly sensing H_2O_2 and GSH. Our fabricated colorimetric sensor shows wide linear ranges for the detection of H_2O_2 (5–150 μmol/L) and GSH (5–50 μmol/L). Its LODs for the detection of H_2O_2 and GSH are as low as 0.19 μmol/L and 0.14 μmol/L, respectively. In the quantitative analysis of H_2O_2 and GSH levels in normal and cancer cells, the colorimetric sensor based on FeS NSs gives high accuracy and reliability. Our study has proven that the prepared 2D FeS NSs are promising for the con-

struction of convenient colorimetric biosensors in medical diagnosis and treatment.

Declaration of competing interest

The authors declare that they have no known competing financial interests or personal relationships that could have appeared to influence the work reported in this paper.

Acknowledgments

This work was financially supported by the Key Grant for Special Professors in Jiangsu Province (No. RK030STP18001), the National Postdoctoral Program for Innovative Talents (No. BX20190156), the China Postdocoral Science Foundation funded project (No. 2021M691654), the "1311 Talents Program" of Nanjing University of Posts and Telecommunications, the Scientific Research Foundation of Nanjing University of Posts and Telecommunications (Nos. NY218150, NY221042).

Supplementary materials

Supplementary material associated with this article can be found, in the online version, at doi:10.1016/j.cclet.2021.10.041.

References

[1] W. Yang, C. Weng, X. Li, et al., Sens. Actuator. B: Chem. 338 (2021) 129844.
[2] T. Peng, X. Dai, Y. Zhang, et al., Sens. Actuator. B: Chem. 304 (2020) 127314.
[3] R. Deng, X. Xie, M. Vendrell, et al., J. Am. Chem. Soc. 133 (2011) 20168–20171.
[4] P. Hou, J. Sun, H. Wang, et al., Sens. Actuator. B: Chem. 304 (2020) 127244.
[5] W. Zhu, G. Jiang, L. Xu, et al., Anal. Chim. Acta 886 (2015) 37–47.
[6] Y. Wang, X. Liu, M. Wang, et al., Sens. Actuator. B: Chem. 329 (2021) 129115.
[7] Y. Zhang, Y. Zhang, X. Xia, et al., Chin. Chem. Lett. 24 (2013) 1053–1058.
[8] H. Liu, Y. Ding, B. Yang, et al., Sens. Actuator. B: Chem. 271 (2018) 336–345.
[9] C. Gao, H. Zhu, J. Chen, H. Qiu, Chin. Chem. Lett. 28 (2017) 1006–1012.
[10] J. Xu, Y. Xing, Y. Liu, et al., Anal. Chim. Acta 1179 (2021) 338825.
[11] H. Huang, J. Zha, S. Li, et al., Chin. Chem. Lett. 33 (2022) 163–176.
[12] Z. Zhou, X. Wang, H. Zhang, et al., Small 17 (2021) 2007486.
[13] Z. Zhou, B. Li, C. Shen, et al., Small 16 (2020) 2004173.
[14] Y. Zhang, H. Du, P. He, et al., Sci. China Mater. 64 (2021) 2613–2623.
[15] Y. Zhang, Q. Shen, Q. Li, et al., Adv. Sci. 8 (2021) 2100386.
[16] Y. Gao, C. Jin, X. Li, et al., Colloids Surf. A 568 (2019) 248–258.
[17] X. Wu, T. Chen, J. Wang, G. Yang, J. Mater. Chem. B 6 (2018) 105–111.
[18] J. Zheng, D. Song, H. Chen, et al., Chin. Chem. Lett. 31 (2020) 1109–1113.
[19] Q. Chen, J. Chen, C. Gao, et al., Analyst 140 (2015) 2857–2863.
[20] L. Huang, W. Zhu, W. Zhang, et al., Mikrochim. Acta 185 (2018) 7.
[21] C. Song, W. Ding, W. Zhao, et al., Biosens. Bioelectron. 151 (2020) 111983.
[22] C. Xie, D. Cen, Z. Ren, et al., Adv. Sci. 7 (2020) 1903512.
[23] X. Zou, Y. Wu, Y. Liu, et al., Chem 4 (2018) 1139–1152.
[24] X. Lai, H. Zhang, Y. Wang, et al., J. Am. Chem. Soc. 32 (2015) 10148–10151.
[25] A.J. Devey, R. Grau-Crespo, N.H. Leeuw, J. Phys. Chem. C 112 (2008) 10960–10967.
[26] G. Genchev, A. Erbe, J. Electrochem. Soc. 163 (2016) C333–C338.
[27] A. Boughriet, R.S. Figueiredo, J. Laureyns, P. Recourt, J. Chem. Soc. Faraday Trans. 93 (1997) 3209–3215.
[28] Y. El Mendili, A. Abdelouas, H. El Hajj, J.F. Bardeau, RSC Adv. 3 (2013) 26343–26351.
[29] T. Yamashita, P. Hayes, Appl. Surf. Sci. 254 (2008) 2441–2449.
[30] M. Mangayayam, K. Dideriksen, M. Ceccato, D.J. Tobler, Environ. Sci. Technol. 53 (2019) 4389–4396.
[31] G. Zhang, P. Wang, W.T. Lu, et al., ACS Appl. Mater. Interfaces 9 (2017) 28566–28576.
[32] Q. Liu, Y. Yang, X. Lv, et al., Sens. Actuator. B: Chem. 240 (2017) 726–734.
[33] P. Roy, Z.H. Lin, C.T. Liang, H.T. Chang, Chem. Commun. 48 (2012) 4079–4081.
[34] Q. Zhang, M. Li, C. Guo, et al., Nanomaterials 9 (2019) 210.
[35] S. Liu, J. Tian, L. Wang, et al., RSC Adv. 2 (2012) 411–413.
[36] S. Cai, Q. Han, C. Qi, et al., Nanoscale 8 (2016) 3685–3693.
[37] W. Shi, Q. Wang, Y. Long, et al., Chem. Commun. 47 (2011) 6695–6697.
[38] C. Liu, S.H. Im, T. Yu, Catalysts 11 (2021) 343.
[39] R.I. Klein Geltink, D. O'Sullivan, E.L. Pearce, Immunity 46 (2017) 525–527.
[40] C. Montfort, N. Matias, A. Fernandez, et al., J. Hepatol. 57 (2012) 852–859.
[41] Y. Ma, Z. Zhang, C. Ren, et al., Analyst 137 (2012) 485–489.
[42] W. Li, J. Wang, J. Zhu, Y.Q. Zheng, J. Mater. Chem. B 6 (2018) 6858–6864.
[43] B. Hu, X. Cao, P. Zhang, New J. Chem. 37 (2013) 3853–3856.
[44] J. Feng, P. Huang, S. Shi, et al., Anal. Chim. Acta 967 (2017) 64–69.
[45] M. Shamsipur, A. Safavi, Z. Mohammadpour, Sens. Actuator. B: Chem. 199 (2014) 463–469.
[46] F. Gong, L. Cheng, N. Yang, et al., Adv. Mater. 31 (2019) 1900730.
[47] L.H. Fu, Y. Wan, C. Qi, et al., Adv. Mater. 33 (2021) 2006892.
[48] G. Qing, X. Zhao, N. Gong, et al., Nat. Commun. 10 (2019) 4336.
[49] B. Xie, X. Yang, R. Zhang, et al., Sens. Actuator. B: Chem. 347 (2021) 130597.
[50] Y. Sun, M. Luo, X. Meng, et al., Anal. Chem. 89 (2017) 3761–3767.
[51] M. Liu, S. Li, D. Huang, et al., Sens. Actuator. B: Chem. 305 (2020) 127512.
[52] H. Jung, X. Chen, J. Kim, et al., Chem. Soc. Rev. 42 (2013) 6019–6031.
[53] T. Du, H. Zhang, J. Ruan, et al., ACS Appl. Mater. Interfaces 10 (2018) 12417–12423.